J. Quant. Spectrosc. Radiat. Transfer. Vol. 11, pp. 1385–1400. Pergamon Press 1971. Printed in Great Britain

EXCITATION OF N_2 AND N_2^+ SYSTEMS BY ELECTRONS—I ABSOLUTE TRANSITION PROBABILITIES

D. E. SHEMANSKY

Department of Physics, University of Pittsburgh, Pittsburgh, Penn. 15213, U.S.A.

and

A. L. BROADFOOT

Kitt Peak National Observatory, Tucson, Arizona 85717, U.S.A.

(*Received* 11 *January* 1971)

Abstract—Quantitative optical measurements of the $N_2 1P, 2P$ and $N_2^+ 1N$ and Meinel systems, excited by electrons, have allowed measurements of transition probabilities, excitation cross-sections, and afterglow effects. This work is reported in two parts. The experiment and observations are described in detail in this article. Absolute transition probabilities have been derived for the $N_2 1P$ and the $N_2^+ M$ systems. Tables of values for the $N_2 2P$ and $N_2^+ 1N$ systems, compiled from earlier measurements, are included to provide a complete set for the four systems.

1. INTRODUCTION

NITROGEN bands are the most prominent features in atmospheric emission spectra and have been studied extensively in the laboratory. However, there is still confusion with regard to some of the absolute transition probabilities, and particularly the electron-excitation cross-sections. Lack of agreement in the recent literature (cf. Part II) brought us to the conclusion that the discrepancies in the laboratory work were probably associated with different techniques employed in making the measurements and the limited scope of individual sets of observations. Therefore, we have measured all of the necessary parameters from a single optical-electron gun system in order to maintain continuity. This approach has been successful, not only in establishing the transition parameters, but in correlating the previous literature.

The purpose of this work was to measure and correlate emission band intensities of the N_2 first positive ($1P$), second positive ($2P$), N_2^+ first negative ($1N$), and Meinel (M) systems excited by electron impact. Since the observations in this experiment were based on emission phenomena, before a study of the excitation mechanisms could be successful, an understanding of the emission characteristics was necessary; the accuracy of optical measurements of relative population rates and total system excitation cross-sections is ultimately limited by the accuracy of the estimated transition probabilities for spontaneous emission. A quantitative discussion of excitation mechanisms would be severely limited

if the populations of excited levels could not be accurately separated from the transition probabilities.

Transition probabilities of the $N_2 2P$ and $N_2^+ 1N$ systems appear to be well established, as we shall discuss below, but this not the case for the $N_2 1P$ and $N_2^+ M$ systems. The present observations have been applied to the estimation of absolute probabilities for the latter systems. This article describes the determination of these values. The experimental arrangements for the measurement of other relevant quantities and details of the observations will also be described below.

Estimates of the relative populations of the excited levels are obtained as a by-product of the analysis of the observed spectra for the determination of transition probabilities. These values, converted into apparent relative population rates, have been examined and utilized in Part II to determine the excitation and deactivation processes affecting the $N_2 1P$ and $N_2^+ M$ excited states. Measurements at various gas pressures, electron energies, and electron currents indicated that there was not a simple relation between the observed relative populations of the vibrational levels and the excitation rate of ground state molecules to these levels. The processes affecting the excited states of both the $N_2 1P$ and $N_2^+ M$ systems could, in fact, not be interpreted without combined steady state and transient measurements. Electron excitation cross-sections of the $N_2 1P$, $2P$ and $N_2^+ M$ systems have been determined relative to the well established $N_2^+ 1N$ cross-section and are presented in Part II.

2. INSTRUMENTATION

A diagram of the collision chamber containing the electron gun is shown in Fig. 1.

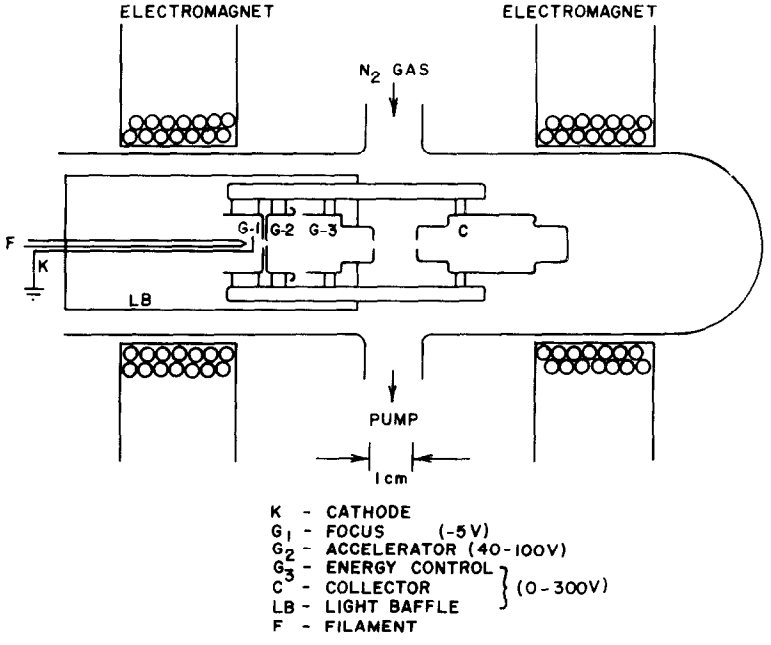

FIG. 1. Electron gun.

The electron beam apparatus was adapted from a television picture tube gun. Some modifications to the electrodes were made to obtain the desired configuration. Radiation from the filament was prevented from illuminating the glassware and beam area by forming a shield of black anodized aluminum around the gun body. The electron beam was collimated with a longitudinal magnetic field generated by coils around the glassware. The gun provided a beam with a diameter of about 1 mm and a peak current of 500 μA. Observations were made in the 1 cm long drift region between the energy control grid and the collector which were at the same potential.

Schematic diagrams of the measurement instrumentation are shown in Figs. 2 and 3. Two grating spectrometers were employed in the observational systems, one as an intensity monitor, and the other as a scanning spectrometer. A $\frac{1}{2}$-m Ebert–Fastie Aerobee flight instrument[1] served as the intensity monitor, and was operated essentially as a tuneable photometer. The detector for this instrument was a cooled[2] EMR 541A (S-11) photomultiplier. The scanning spectrometer[3] was a 1-m Jarrell–Ash model 78–420, coupled to a cooled ITT FW118 (S-1) photomultiplier. At -60°C the dark current from this tube was about 30 count/sec. The grating was moved by a stepping motor through a sine-bar wavelength correction linkage. The detectors and the peripheral apparatus were all operated in the pulse counting mode. An acceptance cone equivalent to about f-3 was established by the imaging optics in front of each spectrometer.

Two recording system configurations were used; one for spectral scanning and one for lifetime measurements.

A. *Spectrum recording system*

The arrangement of the spectrum recording system is shown in Fig. 2. The intensity monitor provided a continuous correction for fluctuations of the beam emission intensity.

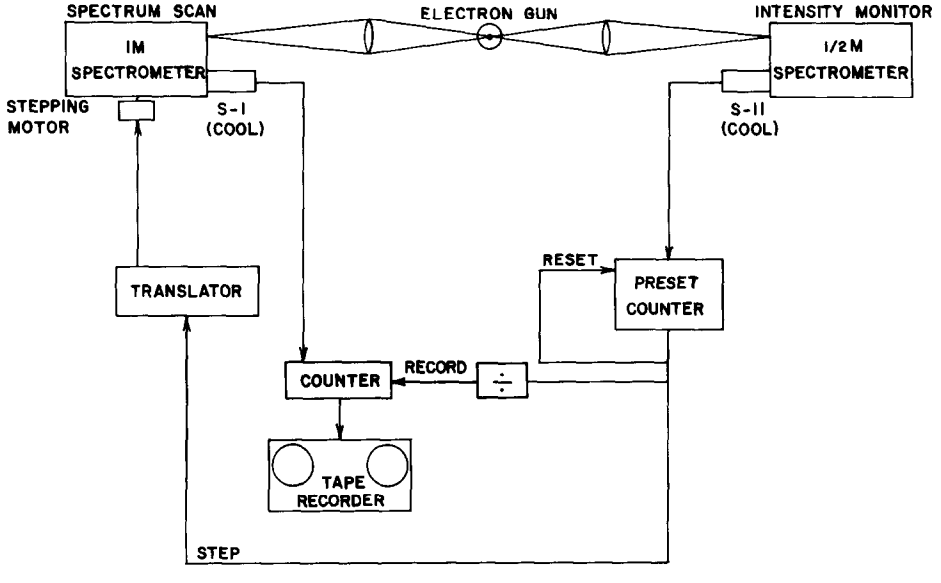

FIG. 2. Experimental arrangement: spectrum scanning system.

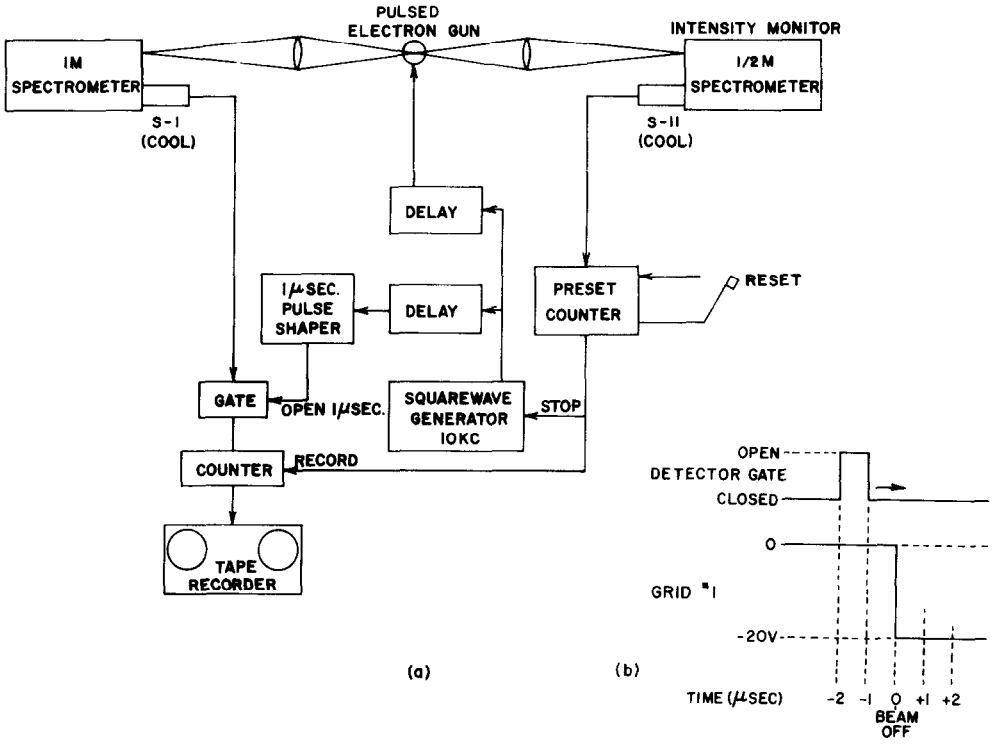

FIG. 3. Experimental arrangement. (a) Lifetime measurement system. (b) Initial phase of beam and detector electronic gates.

The monitor was fixed at the wavelength of a strong band, either the $N_2 1PG$ (6, 3) or $N_2^+ 1N$ (0, 0), for almost all of the measurements. Photoelectron pulses from the monitor were counted into a preset scaler and determined the scan and sample rate of the spectrometer system. Each spectrum was recorded with a single slow scan. The spectra were stored on digital magnetic tape, and analyzed with the aid of a computer.

Calibration[3] of the spectral sensitivity of the 1-m spectrometer was performed by observing a surface of uniform brightness which had been calibrated against a black body. A large calibrated surface was used to fill the field of view of the spectrometer and provide a brightness similar to the observed emission. This emission source was a frosted glass screen back-lighted with a tungsten lamp which was operated at a carefully regulated current. The bulb was separated far enough from the screen to establish essentially uniform brightness over the surface. Under these fixed conditions the surface brightness was calibrated against a black body whose temperature was measured with a standardized thermocouple traceable to N.B.S.

B. *Lifetime recording system*

Lifetimes were determined both by measuring the decay time of the emission after the electron beam was gated off, and by measuring response to a 1 μsec square pulse. Both spectrometers were used in this configuration (Fig. 3(a)). The orientation of the spectro-

meters was such that the beam was perpendicular to the slit direction and the beam was imaged on the entrance slit. The slit, imaged at the beam, was 1 cm long. Again the monitor and preset counter determined exposure time per sample. The beam was turned on and off at a 10 kc rate, and the signal from the spectrometer was sampled with a 1 μsec gate in synchronism with the beam rate. The relative phase of beam and sample gates was continuously variable, so that the response to the driving function could be observed as a function of time. The initial phase of the gates is shown in Fig. 3(b). At the end of each integration interval determined by the monitor, the 1 μsec gate was moved a fraction of a μsec in the direction $+T$ relative to the beam gate for the next sample. A measure of the efficiency of the beam and sample gates was provided by observing the decay of the N_2^+1N (0, 0) band. The lifetime of this emission is short, about 6.6×10^{-8} sec,[4,5] compared to the gate transition times. The shape of the observed buildup and decay curve was compared with the calculated curve for a square gate. The lifetime of this band was detected with low precision which gave us confidence in the system for the lifetimes we were interested in measuring.

3. OBSERVATIONS

In order to estimate the relative population rates and excitation cross-sections of a state, one must first have a measure of the complete set of transition probabilities. This generally requires a combination of experimental measurement and theoretical computation, since in most cases the entire system is not experimentally observable. We regard earlier estimates of the transition probabilities of the N_2^+1N[6] and $N_2 2P$[7] systems as well established values, for reasons which will be pointed out below. The N_2^+M and $N_2 1P$ transition probabilities were not as well determined. The accuracy of the present measurements, coupled with the use of accurate synthetic spectra for data reduction, warranted the re-measurement of these two systems. Observations of the entire 5000–10,500 Å spectral region were therefore conducted to determine a set of transition probability tables. The reduction of the spectra for the determination of transition probabilities automatically yields estimates of the apparent relative population rates ($g_{v'}$) of the upper state vibrational levels. Measurements of $g_{v'}$ were thereby obtained at the same time as a function of pressure, electron energy and current. Once the relative population rates and transition probabilities were determined, the excitation cross-sections were measured by observing selected bands of the $N_2 1P$, $2P$ and N_2^+M systems relative to the well measured N_2^+1N (0, 0) band.

The steady state measurements were accompanied by observations of transient excitation, not only to determine absolute transition probabilities, but to obtain a sensitive measure of processes other than direct excitation and spontaneous emission, affecting the populations of the upper state.

A. *Relative band intensities*

In the case of $N_2 1PG$, five spectra were recorded from 5000 to 10,500 Å at 10 Å spectral half-width. The monitor was set on the $N_2 1PG$ (6, 3) band. The beam current was 10 μA. The pressure and electron energies were,

$P(\mu)$	0.5	2	2	10	10
Energy (eV)	11.5	11.5	17	11.5	17

At 11.5 eV the emission was almost free of cascade from the $C\,^3\Pi_u$ state. At 17.0 eV the cascade contribution to the lower levels of the $B\,^3\Pi_g$ state was evident. This is illustrated in Fig. 4.

The spectrum of the $N_2^+ M$ system was recorded from 6000 to 10,500 Å with a spectral half-width of 10 Å. The monitor was fixed on the $N_2^+ 1N$ (0, 0) band at 3914 Å. One complete spectrum was recorded for each of five pressures and currents with an electron energy of 100 eV.

$P\,(\mu)$	25	11	3	1	0.5
$I\,(\mu A)$	5	12	50	120	130

The spectrum obtained at $P = 3\,\mu$ is reproduced in Fig. 5.

B. *Relative cross-sections of the band systems*

The volume emission rate differs in radial distribution depending on the lifetime and the charge of the excited molecule. For this reason the slit of the scanning spectrometer was oriented perpendicular to the electron beam axis. The slit was 1 cm long and the beam, about 1 mm diameter, was imaged across the center of the slit. Under some conditions we found that $A\,^2\Pi_u$ ions drifted to the walls of the chamber.

Relative intensities were measured for the $N_2^+ 1N$ and M systems at discrete electron energies up to 100 eV and for the $N_2 1P$, $2P$, and $N_2^+ 1N$ systems at lower energies. Finally, the relative emission rates of each system were measured as a function of electron energy, by making observations at small energy intervals while maintaining a constant current.

For the first group, $N_2^+ M$ and $N_2^+ 1NG$, a spectral scan from 7700 to 8050 Å in the first order of the grating gave a good measure of the $N_2^+ M$ (2, 0) band; this same region in the second order, 3850–4025 Å, included the $N_2^+ 1N$ (0, 0) band. It is important to note that the two regions of the spectrum were recorded by changing an order sorting filter. No other change in the system was necessary or in fact allowable if the beam was to be observed under identical conditions in both spectral regions. The spectral half-widths were 10 Å in the first order and 5 Å in the second order. The monitor was fixed on the $N_2^+ 1N$ (0, 0) band. A lifetime measurement of the $N_2^+ M$ (2, 0) band was made under the same conditions for each set of spectra. The following combinations of pressure, current, and electron energy were used in the gun.

$P\,(\mu)$	$I\,(\mu A)$	Energies (eV)
19	8	100, 59, 33
6	8	100, 33
2	50	100, 33

The scan region was moved to 7500–7850 Å for observations of the other group of band systems, $N_2 1PG$, $2PG$, and $N_2^+ 1NG$. The first order spectrum included the $N_2 1P$ (3, 1) and (2, 0) bands, and the second order the $N_2 2P$ (0, 2) and $N_2^+ 1N$ (0, 0) bands. The monitor was fixed on the $N_2 2P$ (0, 0) band at 3373 Å. The spectra were recorded for the following source conditions.

$P\,(\mu)$	$I\,(\mu A)$	Energies (eV)
8	2	32.8, 22.8
1.5	20	31.8, 21.8
0.5	20	31.8, 21.8
0.5	10	31.8

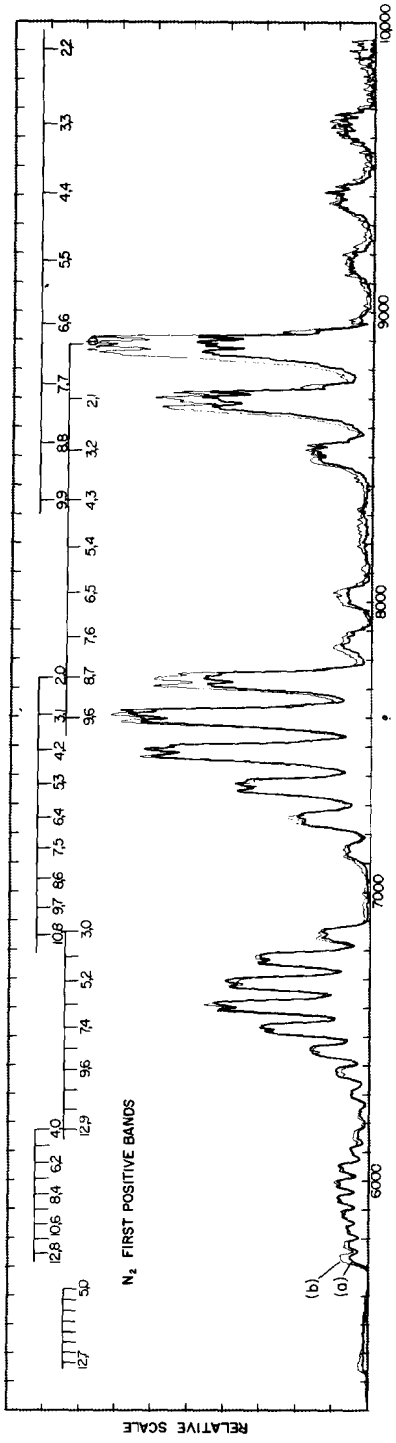

FIG. 4. Experimental spectra N_2 first positive system. 5200–10,000 Å. (a) $P = 2\,\mu$; $E = 11.5$ eV. (b) $P = 10\,\mu$; $E = 17$ eV.

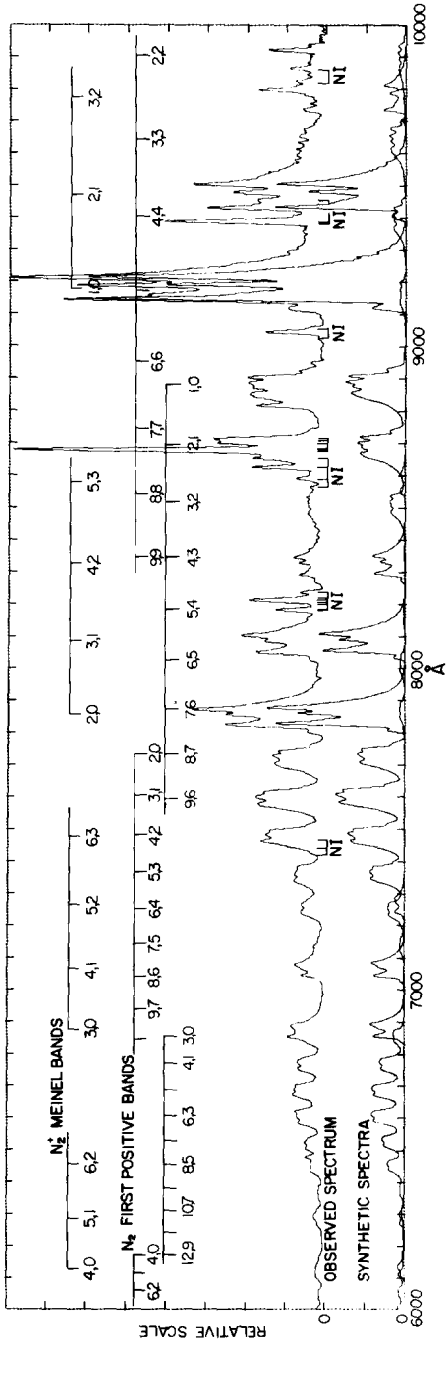

FIG. 5. Experimental and synthetic spectra N_2 first positive and N_2^+ Meinel systems.*
* Experimental spectrum: $P = 3\,\mu$; $E = 100$ eV.

Lifetime measurements of the $N_2 1P$ (3, 1) band were made after the above spectra were recorded because cascade into the $B\,^3\Pi_g$ $v = 3$ level from the $C\,^3\Pi_u$ state could be minimized at lower electron energies. Lifetimes were measured at $E = 12.5$ eV, $P = 0.5$, 9, 50 μ, $I = 3$, 5, and 10 μA. The monitor was fixed on the $N_2 1P$ (6, 3) band.

The relative excitation functions of bands of the four systems, at energies other than the discrete values listed above, were made by varying the electron energy while maintaining a constant electron current and gas pressure, and by using the spectrometer as a photometer rather than a scanning instrument. The electron energy was varied over the range of the gun while control bands from each system were observed, $N_2 1PG$ (3, 1), $2PG$ (0, 0), $N_2^+ 1NG$ (0, 0) and M (2, 0). These curves were put on an absolute scale with the cross-sections determined from the spectra above. Positions of the excitation functions on the energy scale were determined in reference to the threshold of the $N_2^+ 1N$ (0, 0) band.

4. SPECTRAL ANALYSIS AND RESULTS

The volume emission rate for bands of the systems of interest here can be written

$$I_{v'v''} = N_{v'} A_{v'v''} \tag{1}$$

where $N_{v'}$ is the population density of the excited molecules and $A_{v'v''}$ is the spontaneous transition probability of the band. In the steady state, $I_{v'v''}$ can also be written

$$I_{v'v''} = g_{v'} A_{v'v''}/A_{v'}, \tag{2}$$

provided radiationless deactivation can be neglected, where $g_{v'}$ is the population rate, and $A_{v'}$ is related to the natural lifetime, $\tau_{v'}$, of the state by

$$A_{v'} = \sum_{v''} A_{v'v''} = 1/\tau_{v'}. \tag{3}$$

The determination of excitation cross-sections depends on the evaluation of equation (2). The validity of the equation is the subject of considerable discussion in Part II in regard to the $N_2 1P$ and $N_2^+ M$ systems. In particular, we argue that the equation is invalid for the $N_2^+ M$ system at any pressure in the present experiment, and was very likely applied erroneously to all of the previous cross-section work. We do not suggest that equation (2) is invalid for the determination of the *relative* $g_{v'}$ values at any pressure. But even in this case where we do not require an absolute $g_{v'}$, the equation gives erroneous values at all but the lowest pressures for the $N_2^+ M$ system, due to differences in the deactivation rates of the vibrational levels.

Most of the transitions of the observed systems fall into that class, according to the criteria established by FRASER,[8] for which the equation

$$A_{v'v''} = \nu_{v'v''}^3 R_e^2(\bar{r}) q_{v'v''} \tag{4}$$

may be written, where $\nu_{v'v''}$ is the wavenumber, $q_{v'v''}$ is the Franck–Condon factor, $R_e(\bar{r})$ is a measure of the electronic transition moment as a function of internuclear distance and $\bar{r}$ is the r-centroid as defined by Fraser. The Franck–Condon factor is well determined theoretically, but estimates of $R_e(\bar{r})$ are not satisfactory. Experimental steady state measurements of band intensities must be used with equations (1) and (4) to determine $R_e(\bar{r})$. The resulting relative transition probabilities can be placed on an absolute scale using equation

(3) with transient measurements of the natural lifetime. Variations of the method have been used extensively, and are described in detail by Nicholls and his collaborators (Ref. 9).

Band intensities were determined by use of accurate synthetic spectra to separate blended bands.[10,11] In Fig. 5 synthetic spectra are plotted separately for the $N_2 1PG$ and $N_2^+ M$ bands. This shows the overlap of bands of the two systems as well as the blending of adjacent bands of the $N_2 1PG$. When the two synthetic systems were summed, for each wavelength interval, the spectrum was almost identical to the observed spectrum except for atomic emission lines. These synthetic spectra were generated with our final results.

A. *First positive system*

At low electron energies the $N_2 1PG$ can be generated without exciting the $N_2^+ M$ system, which overlaps the $N_2 1PG$, or without exciting the $N_2 2PG$ which cascades into the $N_2 1PG$. This is illustrated in Figs. 4 and 5. Figure 4 curve (a) is the $N_2 1PG$ emission due to 11.5 eV electrons, and is free of contamination. Curve (b) is due to 17 eV electrons and shows the effect of cascade by the $N_2 2PG$. Figure 5 was generated at $E = 100$ eV in the region of the peak production rate of the $N_2^+ M$ system.

An initial synthetic $N_2 1PG$ spectrum was generated using the transition parameters of Ref. (10). The $B\,^3\Pi_g$ vibrational levels were initially assumed to be populated from the N_2 ground state in proportion to the Franck–Condon factors for the ($B\,^3\Pi_g$–$X\,^1\Sigma_g^+$ $v = 0$) transition. Adjustments were made by inspection until a good fit was obtained.

The intensities of the bands in the synthetic spectrum were known accurately and could be easily related to portions of the observed bands. Unblended portions of observed bands and the same portions of the synthetic bands were measured in order to determine the total intensity of the observed bands. Intensities of 32 bands were obtained in this way for the computation of the $R_e(\bar{r})$ curve, Fig. 6, with equations (1), (4). Band intensities from each vibrational level were scaled to give a single smooth $R_e(\bar{r})$ curve; this scaling factor is a measure of the relative population of the vibrational levels, $N_{v'}$.

The lifetime of the $v' = 3$ vibrational level was measured by the decay method described in Section 3 and was found to be $\tau_3 = 6.5\ \mu$sec. This determined $R_e(\bar{r})$ on an absolute scale. The complete set of $A_{v'v''}$-values in Table 1 were then calculated. Franck–Condon factors and $\bar{r}$-values used in the calculations were obtained from ALBRITTON and ZARE[12]; their Franck–Condon factors were similar to those calculated by BENESCH *et al.*[13] Wavelengths listed in Table 1 are calculated band origins.

B. *Meinel system*

The synthetic spectrum in this case was composed of the sum of the $N_2^+ M$ and $N_2 1PG$ with a cascade component of the $N_2 2PG$. A great number of $N_2 1PG$ bands were clear of blends with the $N_2^+ M$ bands which allowed a good fit to the $N_2 1PG$ intensities over the entire spectrum. It was thus possible to predict the $N_2 1PG$ intensity contribution to each wavelength increment through the use of the synthetic spectrum and thereby remove the contribution to the $N_2^+ M$ bands. The synthetic $N_2^+ M$ spectrum was constructed using the data of Ref. (10) to define the rotational structure. The temperature was determined by fitting to a measurement of the (1, 0) band obtained with a spectral half-width of 5 Å. Segments of spectra containing each $N_2^+ M$ band were integrated, and matching sections from the synthetic spectra were used to determine the band intensities. The absolute scale

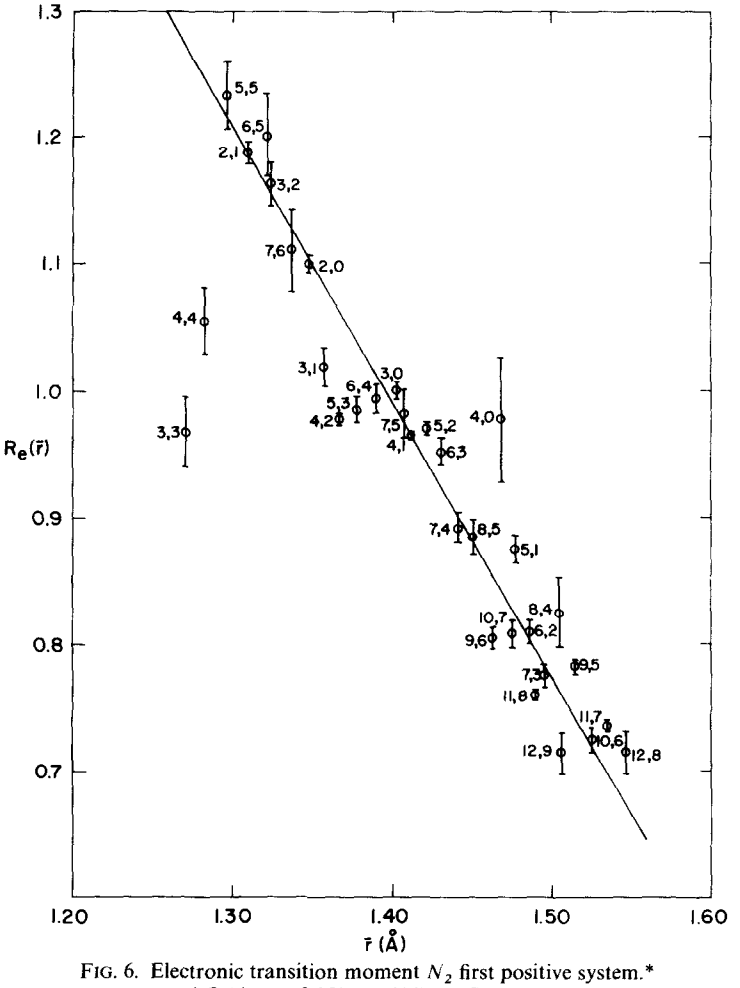

FIG. 6. Electronic transition moment N_2 first positive system.*
* $R_e(\bar{r}) = -2.25(\bar{r}-1.414)+1$. See text.

of $R_e(\bar{r})$ was determined (Fig. 7) from extrapolated lifetime measurements by Ref. (29), rather than from our own estimates. The scale is uncertain and is considered to be an upper limit to the real value. A detailed discussion will be given in Part II. The $A_{v'v''}$ values calculated using the $q_{v'v''}$ and $\bar{r}$ values of Ref. (12), are given in Table 2. The corresponding wavelengths are band origins.

5. DISCUSSION

A. N_2 *Second positive system* ($C\,^3\Pi_u$–$B\,^3\Pi_g$)

Absolute transition probabilities are available for this band system. NICHOLLS[7] used Franck–Condon factors derived from Morse potential models, the intensity measurements of WALLACE and NICHOLLS[14] and the lifetime measurements of BENNETT and DALBY,[4] in his calculations. More recent measurements by TYTE,[15] and also JEUNEHOMME and

TABLE 1. TRANSITION PROBABILITIES OF THE N_2 FIRST POSITIVE SYSTEM

v' \ v''	0	1	2	3	4	5	6	7	8	9	10	11	12	13	$\sum_{v''} A_{v'v''}$	Extrapolated
0	10469.0 6.25+4	12316.6 3.56+4	14894.5 1.12+4	18739.1 2.47+3	25082.9 3.97+2	37522.0 4.24+1									1.12+5	1.12+5
1	8883.4 8.72+4	10179.0 4.12+2	11878.1 1.85+4	14201.7 1.48+4	17569.3 5.69+3	22882.9 1.40+3	32503.7 2.27+2								1.28+5	1.29+5
2	7732.0 4.44+4	8695.3 6.17+4	9905.7 1.25+4	11470.9 2.68+3	13572.1 1.05+4	16538.8 7.29+3	21039.8 2.71+3	28671.4 6.39+2	44417.6 8.87+1						1.42+5	1.43+5
3	6858.3 1.07+4	7605.8 7.73+4	8516.0 2.17+4	9647.7 2.85+4	11092.0 7.97+2	12997.4 3.88+3	15624.1 6.33+3	19473.2 3.68+3	25648.7 1.24+3	37156.2 2.57+2	66089.9 2.54+1				1.54+5	1.54+5
4	6173.1 1.29+3	6772.1 3.02+4	7484.4 8.36+4	8344.7 1.54+3	9403.8 2.94+4	10738.4 7.84+3	12470.6 1.93+2	14806.6 1.52+3	18124.8 3.74+3	23202.8 1.84+3	31932.9 5.44+2	50431.6 9.03+1			1.62+5	1.64+5
5	5621.6 7.42+1	6114.1 5.08+3	6688.7 5.26+4	7367.5 6.86+4	8181.0 3.02+3	9172.9 1.91+4	10407.7 1.52+4	11985.9 1.10+3	14071.2 1.02+3	16951.5 2.81+3	21182.2 2.13+3	27993.4 8.95+2	40756.3 2.24+2		1.72+5	1.73+5
6		5581.6 3.71+2	6056.7 1.19+4	6608.0 7.09+4	7255.0 4.38+4	8024.4 1.58+4	8953.8 7.10+3	10097.6 1.76+4	11538.2 5.11+3	13405.9 —	15920.7 1.40+3	19483.8 1.93+3	24914.0 1.17+3	34170.0 4.24+2	1.78+5	1.81+5
7			5542.7 1.07+3	6000.9 2.14+4	6529.7 8.10+4	7146.5 2.03+4	7874.4 2.88+4	8745.6 5.09+2	9806.0 1.43+4	11123.1 9.39+3	12800.7 1.12+3	15007.4 2.31+2	18035.1 1.26+3	22434.2 1.22+3	1.81+5	1.88+5
8				5504.9 2.34+3	5946.7 3.25+4	6453.9 8.15+4	7041.8 4.94+3	7730.4 3.50+4	8547.4 1.38+3	9531.1 8.11+3	10736.9 1.15+4	12247.4 3.73+3	14191.7 9.33+1	16781.1 4.62+2	1.82+5	1.95+5
9				5092.2 7.77+1	5468.0 4.29+3	5893.9 4.38+4	6380.3 7.31+4	6940.5 —	7592.1 3.28+4	8358.3 7.66+3	9271.4 2.44+3	10376.4 1.04+4	11739.1 6.47+3	13456.6 1.17+3	1.82+5	2.01+5
10					5068.2 1.59+2	5432.0 6.92+3	5842.5 5.38+4	6308.8 5.86+4	6842.6 3.99+3	7458.9 2.44+4	8177.6 1.54+4	9025.3 —	10038.9 6.96+3	11268.9 7.95+3	1.78+5	2.07+5
11						5044.8 2.82+2	5397.0 1.01+4	5792.5 6.11+4	6239.3 4.14+4	6747.7 1.33+4	7330.5 1.38+4	8004.5 2.09+4	8791.8 1.58+3	9721.0 2.98+3	1.65+5	2.13+5
12							5022.1 4.49+2	5362.8 1.38+4	5743.6 6.49+4	6171.7 2.48+4	6655.6 2.37+4	7206.6 4.86+3	7838.5 2.19+4	8568.8 6.03+3	1.60+5	2.18+5

v' \ v'' : λ (Å) / $A_{v'v''}$

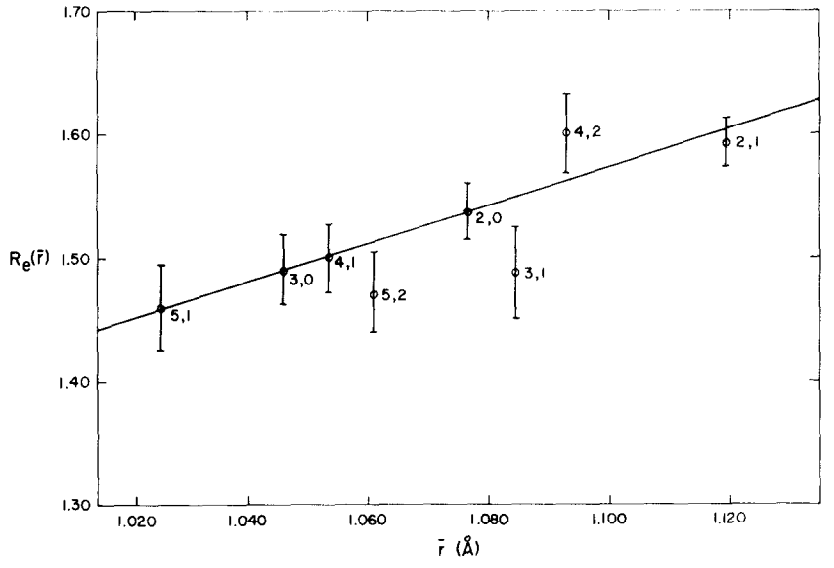

FIG. 7. Electronic transition moment N_2^+ Meinel system.*
* $R_e(\bar{r}) = 1.30(\bar{r} - 0.677) + 1$. See text.

DUNCAN[16] (cf. HESSER[5]), agree well with the intensity measurements and lifetime measurements respectively. In order to bring the NICHOLLS[7] table up to date, the $A_{v'v''}$ values in Table 3 were calculated using the BENESCH *et al.*[13] Franck–Condon factors, the lifetime measurement of BENNETT and DALBY,[4] the $\bar{r}$ values of WALLACE and NICHOLLS,[14] and the TYTE[15] relative intensities. The wavelengths are calculated band origins.

B. N_2^+ *First negative system* ($B\,^2\Sigma_u^+ - X\,^2\Sigma_g^+$)

This system was also treated by NICHOLLS[7] but BROADFOOT[6] could not reproduce his results. Broadfoot has assembled most of the pertinent data on this system and gives a table of absolute parameters. Recent observations of the $N_2^+ 1NG$ (3, 4) band in twilight has required the extension of the previous tabulation. The $A_{v'v''}$ values in Table 4 were calculated using the lifetime measurements of BENNETT and DALBY,[4] $\bar{r}$ values calculated by the mean value method described by NICHOLLS and JARMAIN,[31] $Re(\bar{r})$ values from the equation of WALLACE and NICHOLLS,[14] and NICHOLLS[27] Franck–Condon factors. The wavelengths are calculated band origins.

C. N_2 *First positive system* ($B\,^3\Pi_g - A\,^3\Sigma_u^+$)

Transition probabilities for this system have gone through several modifications. TURNER and NICHOLLS[18] reported band intensities for the $N_2 1PG$ and found the intensity distribution was strongly affected by the electronic transition moment. These measurements were later placed on an absolute scale by NICHOLLS.[9] ZARE, LARSSON and BERG[19] used more accurate Franck–Condon factors with Turner and Nicholls' intensity measurements and concluded that there was no real evidence for variation of $R_e(\bar{r})$. JEUNEHOMME[20] used lifetime measurements of 11 vibrational levels to compute $R_e(\bar{r})$ as a second order

polynomial in $\bar{r}$. The resulting curve was in good agreement with that obtained originally by Turner and Nicholls. Recent calculations of Franck–Condon factors (Ref. 13) based on real potential curves differ somewhat from the old numbers calculated by Nicholls, mainly because of more accurate molecular constants for the $A\ ^3\Sigma_u^+$ state. However, although the new factors changed individual $A_{v'v''}$ values, the $R_e(\bar{r})$ curve remained essentially unchanged.[20] SHEMANSKY and VALLANCE JONES[10] re-calculated the transition probabilities

TABLE 2. TRANSITION PROBABILITIES OF THE N_2^+ MEINEL SYSTEM

v' \ v''	0	1	2	3	4	5	6	7	8	9	τ μsec	$\sum_{v''} A_{v'v''}$
0	11088.4 9.53+4	14612.3 3.34+4	21269.9 3.50+3	38576.5 1.0+2							7.6	1.32+5
1	9182.8 1.011+5	11474.4 7.82+3	15213.8 2.82+4	22402.7 6.10+3	41883.5 2.5+2						7.0	1.43+5
2	7853.6 6.05+4	9471.3 6.93+4	11882.0 2.09+3	15855.7 1.50+4	23636.8 6.78+3	45709.0 3.7+2					6.5	1.54+5
3	6874.4 2.75+4	8082.9 8.61+4	9775.5 2.53+4	12314.5 1.34+4	16544.5 5.14+3	24991.5 5.97+3	50202.9 4.37+2				6.1	1.64+5
4	6123.6 1.08+4	7064.5 6.07+4	8324.1 7.31+4	10096.9 3.03+3	12774.8 1.99+4	17286.2 6.6+2	26486.4 4.43+3	55559.4 4.29+2			5.8	1.73+5
5	5529.8 3.87+3	6285.8 3.24+4	7263.9 7.89+4	8578.1 4.37+4	10436.9 8.7+2	13265.4 1.84+4	18086.5 1.18+2	28142.7 2.81+3	62042.3 3.7+2		5.5	1.82+5
6	5048.7 1.33+3	5671.4 1.48+4	6455.7 5.62+4	7473.3 7.58+4	8845.8 1.73+4	10797.0 7.82+3	13788.6 1.27+4	18951.1 1.36+3	29983.0 1.51+3	70018.3 2.8+2	5.3	1.89+5

v' \ v'' : λ (Å) / $A_{v'v''}$

TABLE 3. TRANSITION PROBABILITIES FOR THE N_2 SECOND POSITIVE SYSTEM

v' \ v''	0	1	2	3	4	5	6	7	8	9	$\tau_{v'}$ sec
0	3370 1.10+7	3576 7.33+6	3804 2.94+6	4058 9.23+5	4343 2.47+5	4665 6.06+4					4.44−8
1	3158 1.02+7	3338 5.28+5	3536 4.61+6	3754 4.10+6	3997 2.49+6	4268 7.69+5	4573 2.35+5	4917 6.74+4			4.35−8
2	2976 3.49+6	3135 8.84+6	3309 5.89+5	3499 1.46+6	3709 3.37+6	3942 2.63+6	4200 1.32+6	4489 5.26+5	4813 1.82+5		4.46−8
3	2818 5.07+5	2961 6.61+6	3115 5.48+6	3284 2.18+6	3468 1.12+5	3671 2.01+6	3894 2.48+6	4140 1.69+6	4415 8.07+5	4722 3.33+5	4.50−8
4	2684 1.85+4	2812 1.33+6	2952 8.64+6	3102 3.24+6	3266 2.01+6	3445 9.12+4	3641 9.11+5	3856 1.95+6	4093 1.73+6	4355 1.01+6	4.78−8

v' \ v'' : $\lambda_{v'v''}$ (Å) / $A_{v'v''}$

TABLE 4. TRANSITION PROBABILITIES FOR THE N_2^+ FIRST NEGATIVE SYSTEM

v' \ v''	0	1	2	3	4	5	$\tau_{v'}$ sec
0	3911.4 1.10+7	4275.1 3.35+6	4706.1 6.75+5	5224.7 1.11+5	5860.4 1.61+4		6.58−8
1	3579.4 6.70+6	3881.6 3.87+6	4233.6 3.81+6	4648.7 1.32+6	5145.3 3.12+6	5749.6 5.90+4	6.22−8
2	3304.9 1.27+6	3560.8 9.16+6	3854.9 8.99+5	4196.0 3.13+6	4596.5 1.71+6	5072.8 5.43+5	5.98−8
3		3295.0 2.98+6	3545.2 9.46+6	3831.7 3.80+4	4162.9 2.18+6	4549.8 1.82+6	5.86−8

v' \ v'' : $\lambda_{v'v''}$ (Å) / $A_{v'v''}$

using the Jeunehomme $R_e(\bar{r})$ curve and the more accurate Franck–Condon factors. The results from the completely new set of observations described here do not differ substantially from the values given by Ref. (10), with the exception of some transitions in the higher v' levels. The present work extends the tables to include the $v' = 12$ level.

The curve for the variation of $R_e(\bar{r})$ with $\bar{r}$, calculated here, is given in Fig. 6. The error bars represent statistical errors in the intensity measurements only. The curve was calculated on the basis of a best fit linear function to all of the measured progressions. The fit to a straight line seems justified; most of the bands lie within 20 per cent of this smooth approximation. The slope is determined by bands from individual upper vibrational levels. Relative populations were derived from the shift required to superpose the $R_e(\bar{r})$ values on a common curve. The apparent relative $g_{v'}$ values determined from the populations are discussed in Part II. A few individual bands deviate markedly from the $R_e(\bar{r})$ curve such as the (4, 4) and (3, 3). There is no suggestion that the entire $v' = 3$ or $v' = 4$, v''-progressions deviate from the general trend since the predicted relative lifetimes of the levels are consistent with the direct measurements as discussed below. Incidents of individual deviation from the general trend of $R_e(\bar{r})$ are not surprising since the method of calculation is approximate and may simply be the consequence of the separation of the electronic and vibrational eigenfunctions.[8]

The relative transition probabilities (Table 1) were placed on an absolute scale with the present lifetime measurement of the $v' = 3$ vibrational level. The lifetimes of the remaining levels were then determined from the summation of the $A_{v'v''}$ values in the table. It was necessary to extrapolate the summations for $v' > 5$ due to the truncation of the Franck–Condon factors at $v'' = 13$. The extrapolated lifetime follows the equation

$$\tau_{v'} = \tau_0/(1+0.542v')^{0.332}. \tag{5}$$

A comparison with other lifetime measurements is shown in Fig. 8. The measurements are in remarkably good agreement, apart from the FOWLER *et al.*[21] values. We wish to emphasize that the relative lifetimes given by Table 1 were determined by steady state

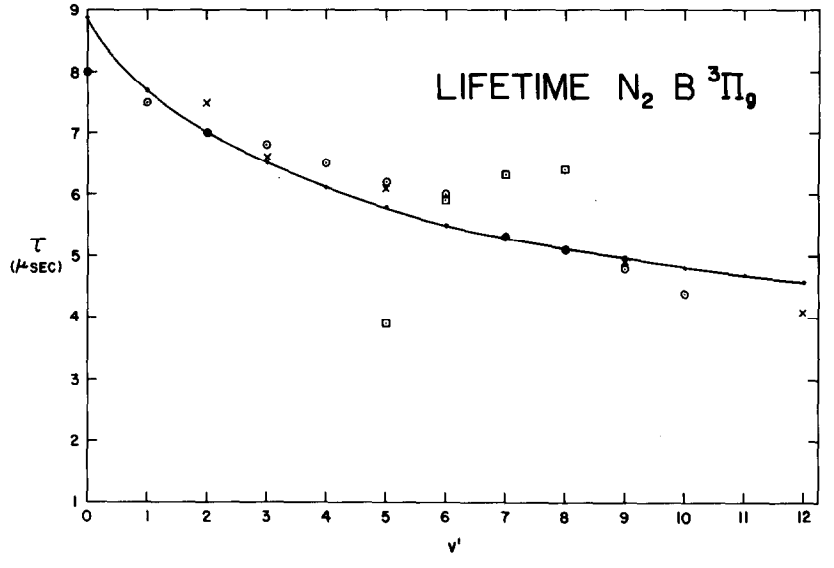

FIG. 8. Lifetimes of the vibrational levels of the N_2 $B\,^3\Pi_g$ state. ——— this work; ⊙ JEUNEHOMME[20]; × HOLLSTEIN *et al.*[30]; ⊡ FOWLER *et al.*[21] See text.

intensity measurements. The good agreement with the directly measured lifetimes suggests that the transition probabilities were well determined, and that the calculated $R_e(\bar{r})$ applied to all of the observed v''-progressions. Some uncertainty would otherwise have been associated with the higher v''-progressions since in those cases as few as 2 bands closely spaced in $\bar{r}$, were available for the estimation of the variation of $R_e(\bar{r})$.

D. N_2^+ *Meinel system* ($A\,^2\Pi_u$–$X\,^2\Sigma_g^+$)

Accurate transition probabilities for this system have not been available, mainly because of a lack of adequate laboratory data. NICHOLLS[22] calculated relative probabilities based on Morse potential Franck–Condon factors,[23] and an electronic transition moment determined from auroral spectra obtained by OMHOLT.[24] NICHOLLS[9] later placed this data on an absolute scale using a crude lifetime estimate by SHERIDAN *et al.*[25] The probabilities were subsequently recalculated by SHEMANSKY,[26] using more accurate Franck–Condon factors[27] based on improved molecular constants.[28] However, the electronic transition moment was determined from the same (Ref. 24) auroral spectra. The Franck–Condon factors (Ref. 12) applied to the present work do not differ significantly from those given by Ref. (27). However the relative transition probabilities (Table 2) differ somewhat from the earlier estimates, presumably because of inaccuracy stemming from the photographic auroral measurements. We consider the use of synthetic spectra for the analysis of these systems essential for the accurate measurement of intensities, even in pure N_2 discharges. The absolute values given in Table 2 differ by an order of magnitude with the Ref. (9) values and by roughly a factor of 3 with Ref. (26). This is due mostly to the present use of more recent lifetime measurements. The difference arising between the Refs. (9, 26) values stems largely from a mistake made by Nicholls in which the transition probability for the (2, 0) band was equated to the natural damping constant for the $v' = 2$ level. How-

ever the present values remain somewhat uncertain. The absolute scale of the numbers in Table 2, as mentioned above, is based on the extrapolated lifetimes measured by O'NEIL and DAVIDSON.[29] The present lifetime measurements and those of Ref. (29) are considered lower limits to the real value. Time of flight measurements by HOLLSTEIN *et al.*[30] ($\tau \doteqdot 12$ μsec) are about a factor of 2 larger than the values in Table 2. The Ref. (30) values should in principle be more accurate than the other estimates, but are not compatible with the present electron cross-section measurements. A detailed discussion of the lifetimes is delayed to Part II, because of their importance to the determination of the excitation cross-sections.

Acknowledgement—The authors wish to thank Dr. D. M. Hunten for his support of the research program. The work was financed partly by Kitt Peak National Observatory, and partly by the University of Pittsburgh.

REFERENCES

1. W. G. FASTIE, *J. opt. Soc. Am.* **42,** 641 (1952).
2. A. L. BROADFOOT, *Appl. Opt.* **5,** 1259 (1966).
3. A. L. BROADFOOT and D. M. HUNTEN, *Can. J. Phys.* **42,** 1212 (1964).
4. R. G. BENNETT and F. W. DALBY, *J. chem. Phys.* **31,** 434 (1959).
5. J. E. HESSER, *J. chem. Phys.* **48,** 2518 (1968).
6. A. L. BROADFOOT, *Planet. Space Sci.* **15,** 1801 (1967).
7. R. W. NICHOLLS, *J. atm. terr. Phys.* **25,** 218 (1963).
8. P. A. FRASER, *Can. J. Phys.* **32,** 515 (1954).
9. R. W. NICHOLLS, *Annal. Geophys.* **20,** 144 (1964).
10. D. E. SHEMANSKY and A. VALLANCE JONES, *Planet. Space Sci.* **16,** 1115 (1968).
11. D. E. SHEMANSKY and N. P. CARLETON, *J. chem. Phys.* **51,** 682 (1969).
12. D. L. ALBRITTON and R. N. ZARE, unpublished.
13. W. BENESCH, J. T. VANDERSLICE, S. G. TILFORD and P. G. WILKINSON, *Astrophys. J.* **144,** 408 (1966).
14. L. V. WALLACE and R. W. NICHOLLS, *J. atm. terr. Phys.* **1,** 101 (1955).
15. D. C. TYTE, *Proc. phys. Soc.* **80,** 1347 (1962).
16. M. JEUNEHOMME and A. B. F. DUNCAN, *J. chem. Phys.* **41,** 1692 (1964).
17. A. L. BROADFOOT, *J. atm. terr. Phys.* **30,** 305 (1968).
18. R. G. TURNER and R. W. NICHOLLS, *Can. J. Phys.* **32,** 468 (1954).
19. R. N. ZARE, E. O. LARSSON and R. A. BERG, *J. molec. Spectry.* **15,** 117 (1965).
20. M. JEUNEHOMME, *J. chem. Phys.* **45,** 1805 (1966).
21. R. G. FOWLER, C. C. LIN and R. M. ST. JOHN, Air Force Weapons Laboratory, Tech. Rep. AFWL-TR-66-132 (1967).
22. R. W. NICHOLLS, *J. atm. terr. Phys.* **12,** 211 (1958).
23. P. A. FRASER, W. R. JARMAIN and R. W. NICHOLLS, *Astrophys. J.* **119,** 286 (1954).
24. A. OMHOLT, *J. atm. terr. Phys.* **10,** 320 (1957).
25. W. F. SHERIDAN, O. OLDENBERG and N. P. CARLETON, *Atomic Collision Processes* (Ed. M. R. C. MCDOWELL). North-Holland, Amsterdam (1964).
26. D. E. SHEMANSKY, Ph.D. Thesis, University of Saskatchewan, Canada (1966).
27. R. W. NICHOLLS, *J. Res. Natn. Bur. Stand.* **65A,** 451 (1961).
28. R. S. MULLIKEN, *The Threshold of Space* (Ed. M. ZELIKOFF). Pergamon Press, New York (1959).
29. R. O'NEIL and G. DAVIDSON, Air Force Cambridge Research Laboratories Tech. Rep. No. AFCRL-67-0277 (1967).
30. M. HOLLSTEIN, D. C. LORENTS, J. R. PETERSON and J. R. SHERIDAN, *Can. J. Chem.* **47,** 1858 (1969).
31. R. W. NICHOLLS and W. R. JARMAIN, *Proc. phys. Soc.* **69,** 253 (1956).